



$K_s^0 K_s^0$ correlations in pp collisions at $\sqrt{s} = 7$ TeV from the LHC ALICE experiment

ALICE Collaboration

ARTICLE INFO

Article history:

Received 12 June 2012
Received in revised form 23 August 2012
Accepted 7 September 2012
Available online 11 September 2012
Editor: M. Doser

ABSTRACT

Identical neutral kaon pair correlations are measured in $\sqrt{s} = 7$ TeV pp collisions in the ALICE experiment. One-dimensional $K_s^0 K_s^0$ correlation functions in terms of the invariant momentum difference of kaon pairs are formed in two multiplicity and two transverse momentum ranges. The femtoscopic parameters for the radius and correlation strength of the kaon source are extracted. The fit includes quantum statistics and final-state interactions of the a_0/f_0 resonance. $K_s^0 K_s^0$ correlations show an increase in radius for increasing multiplicity and a slight decrease in radius for increasing transverse mass, m_T , as seen in $\pi\pi$ correlations in pp collisions and in heavy-ion collisions. Transverse mass scaling is observed between the $K_s^0 K_s^0$ and $\pi\pi$ radii. Also, the first observation is made of the decay of the $f_2(1525)$ meson into the $K_s^0 K_s^0$ channel in pp collisions.

© 2012 CERN. Published by Elsevier B.V. Open access under CC BY-NC-ND license.

1. Introduction

In this Letter we present results from a $K_s^0 K_s^0$ femtoscopy study by the ALICE experiment [1,2] in pp collisions at $\sqrt{s} = 7$ TeV from the CERN LHC. Identical boson femtoscopy, especially identical charged $\pi\pi$ femtoscopy, has been used extensively over the years to study experimentally the space-time geometry of the collision region in high-energy particle and heavy-ion collisions [3]. Recently, the ALICE and CMS collaborations have carried out charged $\pi\pi$ femtoscopic studies for pp collisions at $\sqrt{s} = 7$ TeV [4,5]. These studies show a transverse momentum dependence of the source radius developing with increasing particle multiplicity similar to the one observed in heavy-ion collisions, where the transverse momentum of a particle is defined as $p_T = \sqrt{p_x^2 + p_y^2}$, where p_x and p_y are the components of the particle momentum transverse to the direction of the initial colliding beams. The main motivations to carry out the present $K_s^0 K_s^0$ femtoscopic study to complement this $\pi\pi$ study are 1) to extend the transverse pair momentum range of the charged $\pi\pi$ studies which typically cuts off at about 0.8 GeV/c due to reaching the limit of particle identification, whereas K_s^0 's can easily be identified to 2 GeV/c and beyond, 2) since K_s^0 is uncharged, $K_s^0 K_s^0$ pairs close in phase space are not suppressed by a final-state Coulomb repulsion as is the case of charged $\pi\pi$ pairs, 3) $K_s^0 K_s^0$ pairs close in phase space are additionally enhanced by the strong final-state interaction due to the a_0/f_0 resonance giving a more pronounced signal, and 4) one can, in principle, obtain complementary information about the collision interaction region by using different types of mesons [6–8]. The physics advantage of items 1) and 4) is to study the transverse

mass scaling of the source size which is considered a signature of collective behaviour in heavy-ion collisions [3], where transverse mass is defined as $m_T = \sqrt{p_T^2 + m_0^2}$, where m_0 is the particle rest mass. By definition, m_T scaling occurs when the source sizes from different particle species fall on the same curve vs. m_T . Thus, comparing results from $\pi\pi$ and $K_s^0 K_s^0$ at the same m_T would be a good test of this scaling. Item 3) can be used as an advantage since the final-state interaction of $K_s^0 K_s^0$ via the a_0/f_0 resonance can be calculated with a reasonable degree of precision. Previous $K_s^0 K_s^0$ studies have been carried out in LEP e⁺e⁻ collisions [9–11], HERA ep collisions [12], and RHIC Au-Au collisions [13]. Due to statistics limitations, a single set of femtoscopic source parameters, i.e. radius, R , and correlation strength, λ , was extracted in each of these studies. The present study is the first femtoscopic $K_s^0 K_s^0$ study to be carried out a) in pp collisions and b) in more than one multiplicity and transverse pair momentum, k_T , range, where $k_T = |\vec{p}_{T1} + \vec{p}_{T2}|/2$ and \vec{p}_{T1} and \vec{p}_{T2} are the transverse momenta of the two K_s^0 's from the pair.

2. Description of experiment and data selection

The data analyzed for this work were taken by the ALICE experiment during the 2010 $\sqrt{s} = 7$ TeV pp run at the CERN LHC.

Particle identification and momentum determination were performed with particle tracking in the ALICE Time Projection Chamber (TPC) and ALICE Inner Tracking System (ITS) [1,2]. The TPC was used to record charged-particle tracks as they left ionization trails in the Ne-CO₂ gas. The ionization drifts up to 2.5 m from the central electrode to the end caps to be measured on 159 padrows, which are grouped into 18 sectors; the position at which the track crossed the padrow was determined with resolutions of 2 mm and 3 mm in the drift and transverse directions, respectively. The ITS

* © CERN for the benefit of the ALICE Collaboration.

was used also for tracking. It consists of six silicon layers, two innermost Silicon Pixel Detector (SPD) layers, two Silicon Drift Detector (SDD) layers, and two outer Silicon Strip Detector (SSD) layers, which provide up to six space points for each track. The tracks used in this analysis were reconstructed using the information from both the TPC and the ITS; such tracks were also used to reconstruct the primary vertex of the collision. For details of this procedure and its efficiency see Ref. [2].

A minimum-bias trigger was used for this analysis. Event triggering was accomplished using several sets of detectors. The forward scintillator detectors, VZERO, are placed along the beam line at +3 m and −0.9 m from the nominal interaction point. They cover a region $2.8 < \eta < 5.1$ and $-3.7 < \eta < -1.7$, respectively. They were used in the minimum-bias trigger and their timing signal was used to reject the beam–gas and beam–halo collisions. The minimum-bias trigger required a signal in either of the two VZERO counters or one of the two inner layers of the SPD. Within this sample, events were selected based on the measured charged-particle multiplicity within the pseudorapidity range $|\eta| < 1.2$. Events were required to have a primary vertex within 1 mm of the beam line and 10 cm of the centre of the 5 m long TPC. This provides almost uniform acceptance for particles with $|\eta| < 1$ for all events in the sample. It decreases for $1.0 < |\eta| < 1.2$. In addition, we require events to have at least one charged particle reconstructed within $|\eta| < 1.2$.

Event multiplicity, N_{ch} , was defined as the number of charged particles falling into the pseudorapidity range $|\eta| < 0.8$ and transverse momentum range $0.12 < p_T < 10 \text{ GeV}/c$. The two event multiplicity ranges used in this analysis, 1–11 and >11, correspond to mean charged particle densities, $\langle dN_{\text{ch}}/d\eta \rangle$, of 2.8 and 11.1, respectively, with uncertainties of ∼10%. Events from the Monte Carlo event generator PYTHIA [14,15] were used to estimate $\langle dN_{\text{ch}}/d\eta \rangle$ from the mean charged-particle multiplicity in each range as was done for Table I of Ref. [4], which presents ALICE $\pi\pi$ results for pp collisions at $\sqrt{s} = 7 \text{ TeV}$, event multiplicity having been determined in the same way there as in the present work.

The decay channel $K_s^0 \rightarrow \pi^+\pi^-$ was used for particle identification, with a typical momentum resolution of ∼1% [16]. The distance of closest approach (DCA) of the candidate K_s^0 decay daughters was required to be $\leq 0.1 \text{ cm}$. Fig. 1 shows invariant mass distributions of candidate K_s^0 vertices for the four multiplicity– k_T ranges used in this study (see below) along with a Gaussian + linear fit to the data. The invariant mass at the peaks was found to be $0.497 \text{ GeV}/c^2$, which is within 1 MeV/ c^2 of the accepted mass of the K_s^0 [17]. The average peak width was $\sigma = 3.72 \text{ MeV}/c^2$ demonstrating the good K_s^0 momentum resolution obtained in the ALICE tracking detectors. A vertex was identified with a K_s^0 if the invariant mass of the candidate $\pi^+\pi^-$ pair associated with it fell in the range $0.490\text{--}0.504 \text{ GeV}/c^2$. As seen in Fig. 1, the ratio of the K_s^0 signal to signal + background, $S/(S+B)$, in each of the four ranges is determined to be 0.90 or greater. The minimum K_s^0 flight distance from the primary vertex was 0.5 cm. Additional cuts on the K_s^0 were made in η and p_T , i.e. $|\eta| < 0.8$ and $0.4 < p_T < 3.5 \text{ GeV}/c$. A cut was imposed to prevent $K_s^0 K_s^0$ pairs from sharing the same decay daughter. Minimum bias events with two or more K_s^0 's were selected for use in the analysis. Three or more K_s^0 's occurred in 19% of the events, and all pair combinations of these which satisfied cuts were used.

3. Results

Fig. 2 shows a $K_s^0 K_s^0$ correlation function, $C(Q_{\text{inv}})$, in the invariant momentum difference variable $Q_{\text{inv}} = \sqrt{Q^2 - Q_0^2}$, where Q^2 and Q_0^2 are the squared 3-momentum and energy differences be-

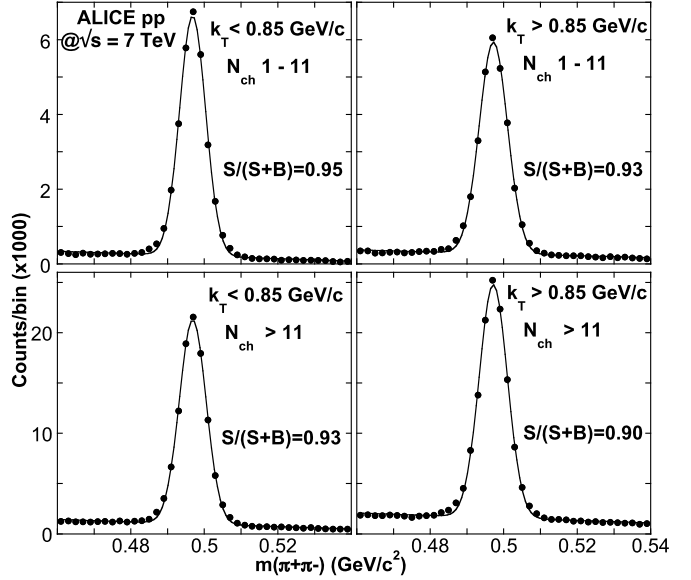


Fig. 1. Invariant mass distributions of $\pi^+\pi^-$ pairs in the four multiplicity– k_T ranges used in the study. K_s^0 used in this analysis were identified by the cut $0.490 \text{ GeV}/c^2 < m < 0.504 \text{ GeV}/c^2$. Also shown is a Gaussian + linear fit to the data points.

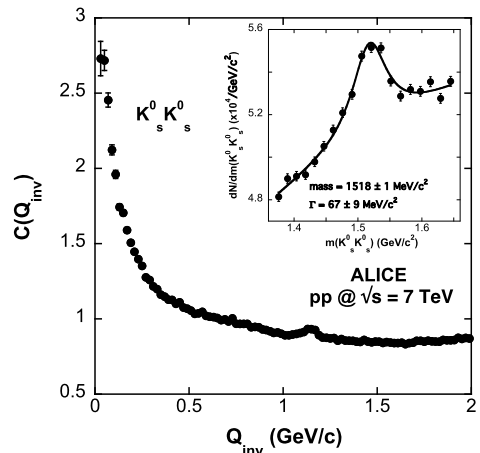


Fig. 2. Inclusive (all event multiplicities and k_T) $K_s^0 K_s^0$ Q_{inv} correlation function. Plotted in the insert to the figure is the invariant $K_s^0 K_s^0$ mass distribution, $dN/dm(K_s^0 K_s^0)$, in the vicinity of the small peak at $Q_{\text{inv}} \approx 1.15 \text{ GeV}/c$.

tween the two particles respectively, for all event multiplicities and k_T . The experimental $C(Q_{\text{inv}})$ is defined as

$$C(Q_{\text{inv}}) = a \frac{N_R(Q_{\text{inv}})}{N_B(Q_{\text{inv}})} \quad (1)$$

where $N_R(Q_{\text{inv}})$ is the number of “real” $K_s^0 K_s^0$ pairs from the same event, $N_B(Q_{\text{inv}})$ is the number of “background” $K_s^0 K_s^0$ pairs constructed by mixing of K_s^0 candidates from ten adjacent events in the same k_T and event multiplicity range as the real pairs, and a is a normalization constant which is adjusted to set the large- Q_{inv} value of $C(Q_{\text{inv}})$ to be in the vicinity of unity. Only events with two or more K_s^0 's were used in event mixing. As a test, background formed using only single- K_s^0 events was found to agree with the default one within the statistical uncertainties. Bins in Q_{inv} were taken to be 20 MeV/c which is greater than the average resolution of Q_{inv} resulting from the experimental momentum resolution. Also, the enhancement region in Q_{inv} of the correlation functions for source sizes of ∼1 fm is ∼200 MeV/c. Thus

the smearing of the correlation function by the experimental momentum resolution has a negligible effect on the present measurements. The three main features seen in this correlation function are 1) a well-defined enhancement region for $Q_{\text{inv}} < 0.3 \text{ GeV}/c$, 2) a non-flat baseline for $Q_{\text{inv}} > 0.3 \text{ GeV}/c$, and 3) a small peak at $Q_{\text{inv}} \approx 1.15 \text{ GeV}/c$.

Considering feature 3) first, fitting a quadratic + Breit-Wigner function to the invariant $K_s^0 K_s^0$ mass distribution, $dN/dm(K_s^0 K_s^0)$, around this peak, where $m(K_s^0 K_s^0) = 2\sqrt{(Q_{\text{inv}}/2)^2 + m_K^2}$, we obtain a mass of $1518 \pm 1 \pm 20 \text{ MeV}/c^2$ and full width (Γ) of $67 \pm 9 \pm 10 \text{ MeV}/c^2$ (giving the statistical and systematic errors, respectively). This is plotted in the insert to Fig. 2. Comparing with the Particle Data Group meson table [17], this peak is a good candidate for the $f_2(1525)$ meson ($m = 1525 \pm 5 \text{ MeV}/c^2$, $\Gamma = 73^{+6}_{-5} \text{ MeV}/c^2$). This is the first observation of the decay of this meson into the $K_s^0 K_s^0$ channel in pp collisions. A similar invariant mass plot to that shown in Fig. 2 was made using PYTHIA for comparison since it contains the $f_2(1525)$ meson. No similar peak was seen above background, thus showing that PYTHIA underestimates the production of this meson in the present system.

In order to disentangle the non-flat baseline from the low- Q_{inv} femtoscopic enhancement, PYTHIA was used to model the baseline. PYTHIA contains neither quantum statistics nor the $K_s^0 K_s^0 \rightarrow a_0/f_0$ channel, but does contain other kinematic effects which could lead to baseline correlations such as mini-jets and momentum and energy conservation effects [4]. PYTHIA events were reconstructed and run through the same analysis method as used for the corresponding experimental data runs to simulate the same conditions as the experimental data analysis. The PYTHIA version of the invariant mass distributions shown for experiment in Fig. 1 yielded similar $S/(S+B)$ values. As a test, the $K_s^0 K_s^0$ background obtained from event mixing using PYTHIA events was compared with that from experiment. Since the background pairs do not have femtoscopic effects, these should ideally be in close agreement. A sample plot of the experimental to PYTHIA ratio of the background vs. Q_{inv} is shown in Fig. 3 for the range $N_{\text{ch}} 1-11$, $k_T < 0.85 \text{ GeV}/c$. The average of the ratio is normalized to unity. It is found that PYTHIA agrees with the Q_{inv} -dependence of the experimental backgrounds within 10%, even though PYTHIA under-predicts the overall scale of $K_s^0 K_s^0$ production by about a factor of 2. Since only ratios of PYTHIA $K_s^0 K_s^0$ distributions are used in disentangling the experimental non-flat baseline, the overall scale factor cancels out. The method of determining the systematic error of using PYTHIA for this purpose is discussed later. The Monte Carlo event generator PHOJET [18,19] was also studied for use in modelling the baseline. When it was compared with the experimental data using the same method shown for PYTHIA in Fig. 3, it was found to not represent the shape of the experimental background as well as PYTHIA, differing from experiment by >20%. It was thus decided to not use PHOJET for this study.

$K_s^0 K_s^0$ correlation functions in Q_{inv} were formed from the data in four ranges: two event multiplicity (1–11, > 11) ranges times two k_T (< 0.85, > 0.85 GeV/c) ranges. About 3×10^8 experimental minimum bias events were analyzed yielding 6×10^6 $K_s^0 K_s^0$ pairs. About 2.3×10^8 PYTHIA minimum bias events used for the baseline determination were also analyzed. This was found to give sufficient statistics for the PYTHIA correlation functions such that the impact of these statistical uncertainties on the measurement of the source parameters was small compared with the systematic uncertainties present in the measurement.

The femtoscopic variables R and λ were extracted in each range by fitting a model correlation function to the double ratio of the experimental correlation function divided by the PYTHIA cor-

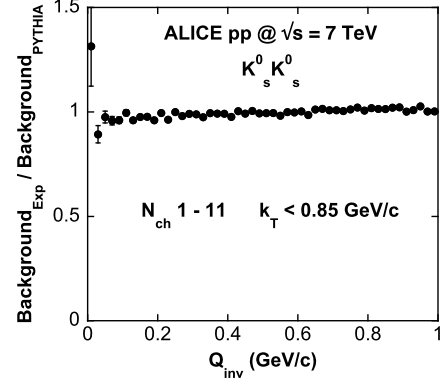


Fig. 3. Ratio of $K_s^0 K_s^0$ experimental background to PYTHIA background vs. Q_{inv} for the range $N_{\text{ch}} 1-11$, $k_T < 0.85 \text{ GeV}/c$. The average of the ratio is normalized to unity.

relation function, $C_{\text{DR}}(Q_{\text{inv}}) = [C(Q_{\text{inv}})]_{\text{exp}}/[C(Q_{\text{inv}})]_{\text{PYTHIA}}$, where $C(Q_{\text{inv}})$ is calculated via the ratio given in Eq. (1). The model correlation function used in the fitting was the Lednicky correlation function [13], $C_L(Q_{\text{inv}})$, based on the model by R. Lednicky and V.L. Lyuboshitz [20]. This model takes into account both quantum statistics and strong final-state interactions from the a_0/f_0 resonance which occur between the $K_s^0 K_s^0$ pair. The K_s^0 spatial distribution is assumed to be Gaussian with a width R in the parametrization and so its influence on the correlation function is from both the quantum statistics and the strong final-state interaction. This is the same parametrization as was used by the RHIC STAR collaboration to extract R and λ from their $K_s^0 K_s^0$ study of Au–Au collisions [13]. The correlation function is

$$C_L(Q_{\text{inv}}) = \lambda C'(Q_{\text{inv}}) + (1 - \lambda) \quad (2)$$

where

$$C'(Q_{\text{inv}}) = 1 + e^{-Q_{\text{inv}}^2 R^2} + \alpha \left[\left| \frac{f(k^*)}{R} \right|^2 + \frac{4 \Re f(k^*)}{\sqrt{\pi} R} F_1(Q_{\text{inv}} R) - \frac{2 \Im f(k^*)}{R} F_2(Q_{\text{inv}} R) \right] \quad (3)$$

and where

$$F_1(z) = \int_0^z dx \frac{e^{x^2 - z^2}}{z}; \quad F_2(z) = \frac{1 - e^{-z^2}}{z}. \quad (4)$$

$f(k^*)$ is the s-wave $K^0 \bar{K}^0$ scattering amplitude whose main contributions are the s-wave isoscalar and isovector f_0 and a_0 resonances [13], R is the radius parameter and λ is the correlation strength parameter (in the ideal case of pure quantum statistics $\lambda = 1$). α is the fraction of $K_s^0 K_s^0$ pairs that come from the $K^0 \bar{K}^0$ system which is set to 0.5 assuming symmetry in K^0 and \bar{K}^0 production [13]. As seen in Eq. (3), the first term is a Gaussian function for quantum statistics and the second term describes the final-state resonance scattering and both are sensitive to the radius parameter, R , giving enhanced sensitivity to this parameter. The scattering amplitude, $f(k^*)$, depends on the resonance masses and decay couplings which have been extracted in various experiments [13]. The uncertainties in these are found to have only a small effect on the extraction of R and λ in the present study. An overall normalization parameter multiplying Eq. (2) is also fit to the experimental correlation function.

Fig. 4 shows the experimental and PYTHIA $K_s^0 K_s^0$ correlation functions for each of the four multiplicity– k_T ranges used. Whereas the experimental correlation functions show an enhancement for

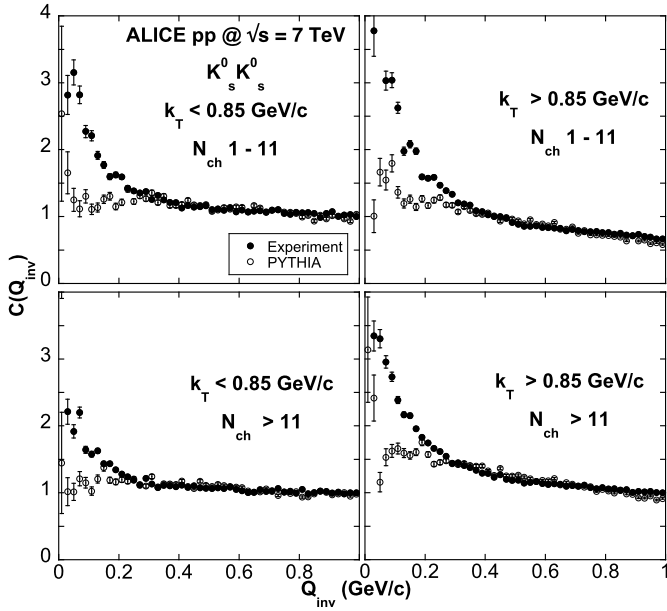


Fig. 4. Experimental and PYTHIA $K_s^0 K_s^0$ correlation functions for the four multiplicity- k_T ranges.

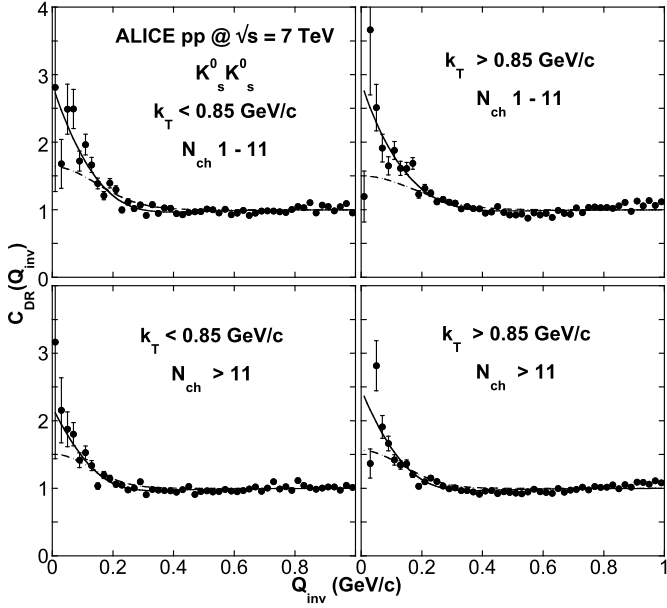


Fig. 5. Experimental $K_s^0 K_s^0$ correlation functions divided by PYTHIA correlation functions for the four multiplicity- k_T ranges with femtoscopic fits using the full Lednicky parametrization (solid lines) and the contribution due to quantum statistics (dashed lines).

$Q_{\text{inv}} < 0.3 \text{ GeV}/c^2$, the PYTHIA correlation functions do not show a similar enhancement. This is what would be expected if the experimental correlation functions contain femtoscopic correlations since PYTHIA does not contain these. PYTHIA is seen to describe the experimental baseline rather well in the region $Q_{\text{inv}} > 0.4 \text{ GeV}/c^2$ where it is expected that effects of femtoscopic correlations are insignificant. Fig. 5 shows $C_{\text{DR}}(Q_{\text{inv}})$, the experimental correlation functions divided by the PYTHIA correlation functions from Fig. 4, along with the fits with the Lednicky parametrization from Eqs. (2)–(4) (solid lines). Also shown for reference is the contribution of the quantum statistics part in Eq. (3) (dashed lines), which are seen to account for roughly one-half of the overall value

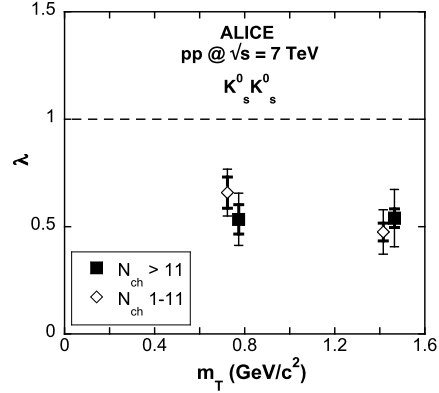


Fig. 6. λ parameters extracted by fitting the Lednicky parametrization to $K_s^0 K_s^0$ correlation functions as shown in Fig. 5. Statistical (darker lines) and total uncertainties are shown. The $N_{\text{ch}} > 11$ points are offset by $0.05 \text{ GeV}/c^2$ for clarity.

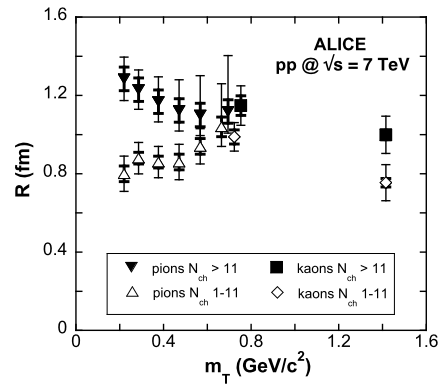


Fig. 7. R parameters extracted by fitting the Lednicky parametrization to $K_s^0 K_s^0$ correlation functions as shown in Fig. 5. Also shown for comparison are R parameters extracted in the same event multiplicity ranges from a $\pi\pi$ femtoscopic study by ALICE [4] in pp collisions at $\sqrt{s} = 7 \text{ TeV}$. Statistical (darker lines) and total uncertainties are shown. The highest m_T pion $N_{\text{ch}} > 11$ point and lower m_T kaon $N_{\text{ch}} > 11$ point have been shifted by $0.03 \text{ GeV}/c^2$ for clarity.

of the correlation functions. The full Lednicky model fits are seen to qualitatively describe the correlation functions within the error bars, which are statistical.

Figs. 6 and 7 and Table 1 present the results of this study for λ and R parameters extracted by fitting the Lednicky parametrization to $K_s^0 K_s^0$ correlation functions as shown in Fig. 5. The source parameters are plotted versus the average $m_T = \sqrt{(k_T)^2 + m_K^2}$ to observe whether m_T scaling is present (as discussed earlier) and statistical + systematic error bars are shown. The statistical uncertainties include both the experimental and the PYTHIA statistical uncertainties used to form the correlation functions, as shown in Fig. 4.

The largest contributions to the systematic uncertainties are 1) the non-statistical uncertainty in using PYTHIA to determine the baseline and 2) the effect of varying the Q_{inv} fit range by $\pm 10\%$. These were found to be on the order of or greater than the size of the statistical uncertainties, as can be seen in Table 1. The method used to estimate the systematic uncertainty of using PYTHIA was to set the PYTHIA $K_s^0 K_s^0$ background distribution equal to the experimental background distribution in the ratio of correlation functions, e.g. forcing the ratio plotted in Fig. 3 to be exactly unity for all Q_{inv} . The ratio of correlation functions then becomes the ratio of the experimental to PYTHIA real pair distributions, which is then fit with the Lednicky parametrization to extract the source parameters. Parameters extracted from these correlation functions were

Table 1

$K_s^0 K_s^0$ source parameters from Lednicky fits for $\sqrt{s} = 7$ TeV pp collisions. Statistical and systematic uncertainties are shown.

k_T range (GeV/c)	N_{ch} range	$\langle k_T \rangle$ (GeV/c)	$\langle dN_{ch}/d\eta \rangle$	λ	R (fm)
< 0.85	1–11	0.52	2.8	$0.66 \pm 0.07 \pm 0.04$	$0.99 \pm 0.04 \pm 0.04$
> 0.85	1–11	1.32	2.8	$0.48 \pm 0.04 \pm 0.06$	$0.75 \pm 0.02 \pm 0.07$
< 0.85	> 11	0.52	11.1	$0.53 \pm 0.07 \pm 0.05$	$1.15 \pm 0.05 \pm 0.05$
> 0.85	> 11	1.32	11.1	$0.54 \pm 0.04 \pm 0.09$	$1.00 \pm 0.02 \pm 0.07$

Table 2

$K_s^0 K_s^0$ source parameters comparing $\alpha = 0.5$ (quantum statistics + FSI) and $\alpha = 0$ (quantum statistics only) fits to Fig. 5 using Eqs. (2)–(4). Statistical uncertainties are shown.

k_T range (GeV/c)	N_{ch} range	λ ($\alpha = 0.5$)	R (fm) ($\alpha = 0.5$)	λ ($\alpha = 0$)	R (fm) ($\alpha = 0$)
< 0.85	1–11	0.64 ± 0.07	0.96 ± 0.04	1.36 ± 0.15	1.35 ± 0.07
> 0.85	1–11	0.50 ± 0.04	0.81 ± 0.02	1.07 ± 0.09	1.05 ± 0.04
< 0.85	> 11	0.51 ± 0.07	1.12 ± 0.05	0.97 ± 0.15	1.64 ± 0.11
> 0.85	> 11	0.56 ± 0.05	1.03 ± 0.02	0.89 ± 0.10	1.37 ± 0.07

then averaged with those from Fig. 5 and are given in Figs. 6 and 7 and Table 1. This method is similar to that used in estimating systematic uncertainties in other $K_s^0 K_s^0$ measurements [10,12]. Other systematic uncertainties were also studied, including the effects of varying the K_s^0 candidate invariant mass acceptance window, using different sets of resonance masses and decay couplings in the scattering amplitude, $f(k^*)$, used in fitting $C_L(Q_{inv})$ in Eq. (3), and momentum resolution effects (as discussed earlier). These were found to be smaller than the statistical uncertainties. The effects of all systematic uncertainties studied on R and λ were added in quadrature to calculate the total systematic uncertainties given in Table 1.

To see the effect of the a_0/f_0 final-state interaction (FSI) term in the Lednicky parametrization, the correlation functions in Fig. 5 were fit with Eqs. (2)–(4) for two cases: 1) quantum statistics + FSI terms, i.e. $\alpha = 0.5$ in Eq. (2), and 2) quantum statistics term only, i.e. $\alpha = 0$ in Eq. (3). Case 2 corresponds to a Gaussian parametrization for R and λ . The results of these fits are shown in Table 2. Including the FSI term in the fit is seen to significantly reduce both R and λ , i.e. R by $\sim 30\%$ and λ by $\sim 50\%$. The FSI is thus seen to enhance the correlation function for $Q_{inv} \rightarrow 0$ making λ appear larger and making the enhancement region narrower. This results in an apparent larger R and λ when fitting with the pure Gaussian quantum statistics model. A reduction in R and λ when including the FSI term was also observed, but to a lesser extent, in the STAR Au–Au $K_s^0 K_s^0$ study [13]. A larger effect of the a_0/f_0 resonance on the correlation function in pp collisions compared with Au–Au collisions is expected since the two kaons are produced in closer proximity to each other in pp collisions, enhancing the probability for final-state interactions.

Within the uncertainties, the m_T dependence of λ is seen in Fig. 6 to be mostly flat with λ lying at an average level of ~ 0.5 –0.6, similar to that found in the ALICE $\pi\pi$ results for pp collisions at $\sqrt{s} = 7$ TeV [4]. In $\pi\pi$ studies the λ value smaller than 1 has been shown at least in part to be due to the presence of long-lived meson resonances which distort the shape of the source so that the Gaussian assumption, which the fitting functions are based on, is less valid [21]. This same explanation is possible for the present λ parameters extracted from the $K_s^0 K_s^0$ correlation functions. For example, the ϕ and K^* mesons with full widths of $\Gamma \sim 4$ and $\Gamma \sim 50$ MeV/ c^2 , respectively, could act as long-lived resonances compared with the extracted source scale of $R \sim 1$ fm, the larger scales being unresolved in the first few Q_{inv} bins but still depressing the overall correlation function.

In Fig. 7 the dependence of the extracted radius parameters on the transverse mass and event multiplicity are shown. Also shown

for comparison are R parameters extracted in the same event multiplicity ranges from a $\pi\pi$ femtoscopic study by ALICE [4] in 7 TeV pp collisions. Looking at the m_T dependence first, the $K_s^0 K_s^0$ results alone suggest a tendency for R to decrease with increasing m_T for both multiplicity ranges. The $\pi\pi$ measurements also show this decreasing trend for the high multiplicity range, but show the opposite trend for the low multiplicity range, R increasing slightly for increasing m_T . Taken with the $\pi\pi$ results the $K_s^0 K_s^0$ results for R extend the covered range of m_T to ~ 1.3 GeV/c, which is more than twice the range as for $\pi\pi$. The lower m_T points for $K_s^0 K_s^0$ which are in close proximity in m_T to the highest m_T points for $\pi\pi$ are seen to overlap within errors, showing m_T scaling. The m_T dependence of R combining both particle species is seen to be weak or non-existent within the error bars. Looking at the multiplicity dependence, a tendency for R to increase overall for increasing event multiplicity is seen for both $\pi\pi$ and $K_s^0 K_s^0$ measurements as is observed in $\pi\pi$ heavy-ion collision studies [22].

The multiplicity– m_T dependence of the pion femtoscopic radii in heavy-ion collisions is interpreted as a signature for collective hydrodynamic matter behaviour [3]. Such dependences have also been discussed in e^+e^- collisions [23,24]. The corresponding measurements in pp collisions at $\sqrt{s} = 7$ TeV also show a multiplicity– m_T dependence [4,5]. However, important differences with heavy-ion collisions remain, for example at low multiplicities the pion R seems to increase with increasing m_T rather than decreasing as with heavy-ion collisions, as already mentioned earlier. The interpretation of these pp results for pions is still not clear, although model calculations exist that attempt to explain them via a collective phase created in high-multiplicity pp collisions [25–27]. If such a collective phase is hydrodynamic-like, the m_T dependence of the radii should extend to heavier particles such as the K_s^0 as well, as shown in Ref. [27]. The measurements presented in this Letter provide a cross-check of the collectivity hypothesis. The interpretation is, however, complicated by the fact that in such small systems particles coming from the decay of strong resonances play a significant role [28]; simple chemical model calculations show that this influence should be relatively smaller for kaons than for pions. So far, no model calculations are known in the literature for any KK correlations in pp collisions for $m_T \geq 0.7$ GeV/ c^2 , but the results measured in the present study should act as a motivation for such calculations.

4. Summary

In summary, identical neutral kaon pair correlations have been measured in $\sqrt{s} = 7$ TeV pp collisions in the ALICE experiment. One-dimensional $K_s^0 K_s^0$ correlation functions in terms of

the invariant momentum difference of kaon pairs were formed in two multiplicity and two transverse momentum ranges. The femtoscopic kaon source parameters R and λ have been extracted. The fit includes quantum statistics and final-state interactions of the a_0/f_0 resonance. $K_s^0 K_s^0$ correlations show an increase in R for increasing multiplicity and a slight decrease in R for increasing m_T as seen in $\pi\pi$ correlations in the pp system and in heavy-ion collisions. Within uncertainties, m_T scaling is also observed for the $K_s^0 K_s^0$ and $\pi\pi$ radii.

Acknowledgements

The ALICE collaboration would like to thank all its engineers and technicians for their invaluable contributions to the construction of the experiment and the CERN accelerator teams for the outstanding performance of the LHC complex.

The ALICE collaboration acknowledges the following funding agencies for their support in building and running the ALICE detector:

Calouste Gulbenkian Foundation from Lisbon and Swiss Fonds Kidagan, Armenia;

Conselho Nacional de Desenvolvimento Científico e Tecnológico (CNPq), Financiadora de Estudos e Projetos (FINEP), Fundação de Amparo à Pesquisa do Estado de São Paulo (FAPESP);

National Natural Science Foundation of China (NSFC), the Chinese Ministry of Education (CMOE) and the Ministry of Science and Technology of China (MSTC);

Ministry of Education and Youth of the Czech Republic;

Danish Natural Science Research Council, the Carlsberg Foundation and the Danish National Research Foundation;

The European Research Council under the European Community's Seventh Framework Programme;

Helsinki Institute of Physics and the Academy of Finland;

French CNRS-IN2P3, the 'Region Pays de Loire', 'Region Alsace', 'Region Auvergne' and CEA, France;

German BMBF and the Helmholtz Association;

General Secretariat for Research and Technology, Ministry of Development, Greece;

Hungarian OTKA and National Office for Research and Technology (NKTH);

Department of Atomic Energy and Department of Science and Technology of the Government of India;

Istituto Nazionale di Fisica Nucleare (INFN) of Italy;

MEXT Grant-in-Aid for Specially Promoted Research, Japan;

Joint Institute for Nuclear Research, Dubna;

National Research Foundation of Korea (NRF);

CONACYT, DGAPA, México, ALFA-EC and the HELEN Program (High-Energy physics Latin-American-European Network);

Stichting voor Fundamenteel Onderzoek der Materie (FOM) and the Nederlandse Organisatie voor Wetenschappelijk Onderzoek (NWO), Netherlands;

Research Council of Norway (NFR);

Polish Ministry of Science and Higher Education;

National Authority for Scientific Research – NASR (Autoritatea Națională pentru Cercetare Științifică – ANCS);

Federal Agency of Science of the Ministry of Education and Science of Russian Federation, International Science and Technology Center, Russian Academy of Sciences, Russian Federal Agency of Atomic Energy, Russian Federal Agency for Science and Innovations and CERN-INTAS;

Ministry of Education of Slovakia;

Department of Science and Technology, South Africa;

CIEMAT, EELA, Ministerio de Educación y Ciencia of Spain, Xunta de Galicia (Consellería de Educación), CEADEN, Cubaenergía, Cuba, and IAEA (International Atomic Energy Agency);

Swedish Research Council (VR) and Knut & Alice Wallenberg Foundation (KAW);

Ukraine Ministry of Education and Science;

United Kingdom Science and Technology Facilities Council (STFC);

The United States Department of Energy, the United States National Science Foundation, the State of Texas, and the State of Ohio.

Open access

This article is published Open Access at sciencedirect.com. It is distributed under the terms of the Creative Commons Attribution License 3.0, which permits unrestricted use, distribution, and reproduction in any medium, provided the original authors and source are credited.

References

- [1] K. Aamodt, et al., ALICE Collaboration, JINST 3 (2008) S08002.
- [2] K. Aamodt, et al., ALICE Collaboration, Eur. Phys. J. C 68 (2010) 345.
- [3] M.A. Lisa, S. Pratt, R. Soltz, U. Wiedemann, Ann. Rev. Nucl. Part. Sci. 55 (2005) 357.
- [4] K. Aamodt, et al., ALICE Collaboration, Phys. Rev. D 84 (2011) 112004, arXiv:1101.3665.
- [5] V. Khachatryan, et al., CMS Collaboration, JHEP 1105 (2011) 029, arXiv: 1101.3518 [hep-ex].
- [6] H.J. Lipkin, Phys. Lett. B 219 (1989) 474.
- [7] H.J. Lipkin, Phys. Rev. Lett. 69 (1992) 3700, hep-ph/9212255.
- [8] G. Alexander, H.J. Lipkin, Phys. Lett. B 456 (1999) 270, hep-ph/9903205.
- [9] P. Abreu, et al., DELPHI Collaboration, Phys. Lett. B 379 (1996) 330.
- [10] S. Schael, et al., ALEPH Collaboration, Phys. Lett. B 611 (2005) 66.
- [11] G. Abbiendi, et al., OPAL Collaboration, Eur. J. Phys. C 21 (2001) 23.
- [12] S. Chekanov, et al., ZEUS Collaboration, Phys. Lett. B 652 (2007) 1.
- [13] B.I. Abelev, et al., STAR Collaboration, Phys. Rev. C 74 (2006) 054902.
- [14] T. Sjöstrand, L. Lonnblad, S. Mrenna, P. Skands, hep-ph/0603175, March 2006.
- [15] P.Z. Skands, arXiv:0905.3418, 2009.
- [16] K. Aamodt, et al., ALICE Collaboration, Eur. Phys. J. C 71 (2011) 1594, arXiv: 1012.3257 [hep-ex].
- [17] K. Nakamura, et al., Particle Data Group, J. Phys. G 37 (2010) 075021.
- [18] R. Engel, Z. Phys. C 66 (1995) 203.
- [19] R. Engel, J. Ranft, Phys. Rev. D 54 (1996) 4244, hep-ph/9509373.
- [20] R. Lednický, V.L. Lyuboshitz, Sov. J. Nucl. Phys. 35 (1982) 770.
- [21] T.J. Humanic, Phys. Rev. C 76 (2007) 025205.
- [22] K. Aamodt, et al., ALICE Collaboration, Phys. Lett. B 696 (2011) 328, arXiv:1012.4035 [nucl-ex].
- [23] A. Bialas, M. Kucharczyk, H. Palka, K. Zalewski, Phys. Rev. D 62 (2000) 114007, hep-ph/0006290.
- [24] A. Bialas, K. Zalewski, Acta Phys. Polon. B 30 (1999) 359, hep-ph/9901382.
- [25] P. Bozek, Acta Phys. Polon. B 41 (2010) 837, arXiv:0911.2392 [nucl-th].
- [26] K. Werner, K. Mikhailov, I. Karpenko, T. Pierog, arXiv:1104.2405 [hep-ph].
- [27] D. Truesdale, T.J. Humanic, J. Phys. G: Nucl. Part. Phys. 39 (2012) 015011.
- [28] A. Kisiel, Phys. Rev. C 84 (2011) 044913, arXiv:1012.1517 [nucl-th].

ALICE Collaboration

B. Abelev ⁶⁸, J. Adam ³³, D. Adamová ⁷³, A.M. Adare ¹²⁰, M.M. Aggarwal ⁷⁷, G. Aglieri Rinella ²⁹, A.G. Agocs ⁶⁰, A. Agostinelli ²¹, S. Aguilar Salazar ⁵⁶, Z. Ahmed ¹¹⁶, A. Ahmad Masoodi ¹³, N. Ahmad ¹³, S.A. Ahn ⁶², S.U. Ahn ^{63,36}, A. Akindinov ⁴⁶, D. Aleksandrov ⁸⁸, B. Alessandro ⁹⁴, R. Alfaro Molina ⁵⁶, A. Aalic ^{97,9}, A. Alkin ², E. Almaráz Aviña ⁵⁶, J. Alme ³¹, T. Alt ³⁵, V. Altini ²⁷, S. Altinpinar ¹⁴,

- I. Altsybeev ¹¹⁷, C. Andrei ⁷⁰, A. Andronic ⁸⁵, V. Anguelov ⁸², J. Anielski ⁵⁴, C. Anson ¹⁵, T. Antićić ⁸⁶, F. Antinori ⁹³, P. Antonioli ⁹⁷, L. Aphecetche ¹⁰², H. Appelshäuser ⁵², N. Arbor ⁶⁴, S. Arcelli ²¹, A. Arend ⁵², N. Armesto ¹², R. Arnaldi ⁹⁴, T. Aronsson ¹²⁰, I.C. Arsene ⁸⁵, M. Arslanbekov ⁵², A. Asryan ¹¹⁷, A. Augustinus ²⁹, R. Averbeck ⁸⁵, T.C. Awes ⁷⁴, J. Äystö ³⁷, M.D. Azmi ¹³, M. Bach ³⁵, A. Badalà ⁹⁹, Y.W. Baek ^{63,36}, R. Bailhache ⁵², R. Bala ⁹⁴, R. Baldini Ferroli ⁹, A. Baldissari ¹¹, A. Baldit ⁶³, F. Baltasar Dos Santos Pedrosa ²⁹, J. Bán ⁴⁷, R.C. Baral ⁴⁸, R. Barbera ²³, F. Barile ²⁷, G.G. Barnaföldi ⁶⁰, L.S. Barnby ⁹⁰, V. Barret ⁶³, J. Bartke ¹⁰⁴, M. Basile ²¹, N. Bastid ⁶³, S. Basu ¹¹⁶, B. Bathen ⁵⁴, G. Batigne ¹⁰², B. Batyunya ⁵⁹, C. Baumann ⁵², I.G. Bearden ⁷¹, H. Beck ⁵², I. Belikov ⁵⁸, F. Bellini ²¹, R. Bellwied ¹¹⁰, E. Belmont-Moreno ⁵⁶, G. Bencedi ⁶⁰, S. Beole ²⁵, I. Berceanu ⁷⁰, A. Bercuci ⁷⁰, Y. Berdnikov ⁷⁵, D. Berenyi ⁶⁰, A.A.E. Bergognon ¹⁰², D. Berzana ⁹⁴, L. Betev ²⁹, A. Bhasin ⁸⁰, A.K. Bhati ⁷⁷, J. Bhom ¹¹⁴, L. Bianchi ²⁵, N. Bianchi ⁶⁵, C. Bianchin ¹⁹, J. Bielčík ³³, J. Bielčíková ⁷³, A. Bilandžić ^{72,71}, S. Bjelogrlic ⁴⁵, F. Blanco ⁷, F. Blanco ¹¹⁰, D. Blau ⁸⁸, C. Blume ⁵², M. Boccioli ²⁹, N. Bock ¹⁵, S. Böttger ⁵¹, A. Bogdanov ⁶⁹, H. Bøggild ⁷¹, M. Bogolyubsky ⁴³, L. Boldizsár ⁶⁰, M. Bombara ³⁴, J. Book ⁵², H. Borel ¹¹, A. Borissov ¹¹⁹, S. Bose ⁸⁹, F. Bossú ²⁵, M. Botje ⁷², B. Boyer ⁴², E. Braidot ⁶⁷, P. Braun-Munzinger ⁸⁵, M. Bregant ¹⁰², T. Breitner ⁵¹, T.A. Browning ⁸³, M. Broz ³², R. Brun ²⁹, E. Bruna ^{25,94}, G.E. Bruno ²⁷, D. Budnikov ⁸⁷, H. Buesching ⁵², S. Bufalino ^{25,94}, K. Bugaiev ², O. Busch ⁸², Z. Buthelezi ⁷⁹, D. Caballero Orduna ¹²⁰, D. Caffarri ¹⁹, X. Cai ³⁹, H. Caines ¹²⁰, E. Calvo Villar ⁹¹, P. Camerini ²⁰, V. Canoa Roman ⁸, G. Cara Romeo ⁹⁷, F. Carena ²⁹, W. Carena ²⁹, N. Carlin Filho ¹⁰⁷, F. Carminati ²⁹, C.A. Carrillo Montoya ²⁹, A. Casanova Díaz ⁶⁵, J. Castillo Castellanos ¹¹, J.F. Castillo Hernandez ⁸⁵, E.A.R. Casula ¹⁸, V. Catanescu ⁷⁰, C. Cavicchioli ²⁹, C. Ceballos Sanchez ⁶, J. Cepila ³³, P. Cerello ⁹⁴, B. Chang ^{37,123}, S. Chapelard ²⁹, J.L. Charvet ¹¹, S. Chattopadhyay ¹¹⁶, S. Chattopadhyay ⁸⁹, I. Chawla ⁷⁷, M. Cherney ⁷⁶, C. Cheshkov ^{29,109}, B. Cheynis ¹⁰⁹, V. Chibante Barroso ²⁹, D.D. Chinellato ¹⁰⁸, P. Chochula ²⁹, M. Chojnacki ⁴⁵, S. Choudhury ¹¹⁶, P. Christakoglou ^{72,45}, C.H. Christensen ⁷¹, P. Christiansen ²⁸, T. Chujo ¹¹⁴, S.U. Chung ⁸⁴, C. Cicalo ⁹⁶, L. Cifarelli ^{21,29,9}, F. Cindolo ⁹⁷, J. Cleymans ⁷⁹, F. Coccetti ⁹, F. Colamaria ²⁷, D. Colella ²⁷, G. Conesa Balbastre ⁶⁴, Z. Conesa del Valle ²⁹, P. Constantin ⁸², G. Contin ²⁰, J.G. Contreras ⁸, T.M. Cormier ¹¹⁹, Y. Corrales Morales ²⁵, P. Cortese ²⁶, I. Cortés Maldonado ¹, M.R. Cosentino ⁶⁷, F. Costa ²⁹, M.E. Cotallo ⁷, E. Crescio ⁸, P. Crochet ⁶³, E. Cruz Alaniz ⁵⁶, E. Cuautle ⁵⁵, L. Cunqueiro ⁶⁵, A. Dainese ^{19,93}, H.H. Dalsgaard ⁷¹, A. Danu ⁵⁰, D. Das ⁸⁹, I. Das ⁴², K. Das ⁸⁹, S. Dash ⁴⁰, A. Dash ¹⁰⁸, S. De ¹¹⁶, G.O.V. de Barros ¹⁰⁷, A. De Caro ^{24,9}, G. de Cataldo ⁹⁸, J. de Cuveland ³⁵, A. De Falco ¹⁸, D. De Gruttola ²⁴, H. Delagrange ¹⁰², A. Deloff ¹⁰⁰, V. Demanov ⁸⁷, N. De Marco ⁹⁴, E. Dénes ⁶⁰, S. De Pasquale ²⁴, A. Deppmann ¹⁰⁷, G. D’Erasio ²⁷, R. de Rooij ⁴⁵, M.A. Diaz Corchero ⁷, D. Di Bari ²⁷, T. Dietel ⁵⁴, S. Di Liberto ⁹⁵, A. Di Mauro ²⁹, P. Di Nezza ⁶⁵, R. Divià ²⁹, Ø. Djupsland ¹⁴, A. Dobrin ^{119,28}, T. Dobrowolski ¹⁰⁰, I. Domínguez ⁵⁵, B. Dönigus ⁸⁵, O. Dordic ¹⁷, O. Driga ¹⁰², A.K. Dubey ¹¹⁶, L. Ducroux ¹⁰⁹, P. Dupieux ⁶³, M.R. Dutta Majumdar ¹¹⁶, A.K. Dutta Majumdar ⁸⁹, D. Elia ⁹⁸, D. Emschermann ⁵⁴, H. Engel ⁵¹, H.A. Erdal ³¹, B. Espagnon ⁴², M. Estienne ¹⁰², S. Esumi ¹¹⁴, D. Evans ⁹⁰, G. Eyyubova ¹⁷, D. Fabris ^{19,93}, J. Faivre ⁶⁴, D. Falchieri ²¹, A. Fantoni ⁶⁵, M. Fasel ⁸⁵, R. Fearick ⁷⁹, A. Fedunov ⁵⁹, D. Fehlker ¹⁴, L. Feldkamp ⁵⁴, D. Feleac ⁵⁰, B. Fenton-Olsen ⁶⁷, G. Feofilov ¹¹⁷, A. Fernández Téllez ¹, A. Ferretti ²⁵, R. Ferretti ²⁶, J. Figiel ¹⁰⁴, M.A.S. Figueiredo ¹⁰⁷, S. Filchagin ⁸⁷, D. Finogeev ⁴⁴, F.M. Fionda ²⁷, E.M. Fiore ²⁷, M. Floris ²⁹, S. Foertsch ⁷⁹, P. Foka ⁸⁵, S. Fokin ⁸⁸, E. Fragiaco ⁹², U. Frankenfeld ⁸⁵, U. Fuchs ²⁹, C. Furget ⁶⁴, M. Fusco Girard ²⁴, J.J. Gaardhøje ⁷¹, M. Gagliardi ²⁵, A. Gago ⁹¹, M. Gallio ²⁵, D.R. Gangadharan ¹⁵, P. Ganoti ⁷⁴, C. Garabatos ⁸⁵, E. Garcia-Solis ¹⁰, I. Garishvili ⁶⁸, J. Gerhard ³⁵, M. Germain ¹⁰², C. Geuna ¹¹, A. Gheata ²⁹, M. Gheata ^{50,29}, B. Ghidini ²⁷, P. Ghosh ¹¹⁶, P. Gianotti ⁶⁵, M.R. Girard ¹¹⁸, P. Giubellino ²⁹, E. Gladysz-Dziadus ¹⁰⁴, P. Glässsel ⁸², R. Gomez ¹⁰⁶, A. Gonschior ⁸⁵, E.G. Ferreira ¹², L.H. González-Trueba ⁵⁶, P. González-Zamora ⁷, S. Gorbunov ³⁵, A. Goswami ⁸¹, S. Gotovac ¹⁰³, V. Grabski ⁵⁶, L.K. Graczykowski ¹¹⁸, R. Grajcarek ⁸², A. Grelli ⁴⁵, C. Grigoras ²⁹, A. Grigoras ²⁹, V. Grigoriev ⁶⁹, A. Grigoryan ¹²¹, S. Grigoryan ⁵⁹, B. Grinyov ², N. Grion ⁹², P. Gros ²⁸, J.F. Grosse-Oetringhaus ²⁹, J.-Y. Grossiord ¹⁰⁹, R. Grossiord ²⁹, F. Guber ⁴⁴, R. Guernane ⁶⁴, C. Guerra Gutierrez ⁹¹, B. Guerzoni ²¹, M. Guilbaud ¹⁰⁹, K. Gulbrandsen ⁷¹, T. Gunji ¹¹³, A. Gupta ⁸⁰, R. Gupta ⁸⁰, H. Gutbrod ⁸⁵, Ø. Haaland ¹⁴, C. Hadjidakis ⁴², M. Haiduc ⁵⁰, H. Hamagaki ¹¹³, G. Hamar ⁶⁰, B.H. Han ¹⁶, L.D. Hanratty ⁹⁰, A. Hansen ⁷¹, Z. Harmanova ³⁴, J.W. Harris ¹²⁰, M. Hartig ⁵², D. Hasegan ⁵⁰, D. Hatzifotiadou ⁹⁷, A. Hayrapetyan ^{29,121}, S.T. Heckel ⁵², M. Heide ⁵⁴, H. Helstrup ³¹, A. Hergelegiu ⁷⁰, G. Herrera Corral ⁸, N. Herrmann ⁸², B.A. Hess ¹¹⁵, K.F. Hetland ³¹, B. Hicks ¹²⁰,

- P.T. Hille¹²⁰, B. Hippolyte⁵⁸, T. Horaguchi¹¹⁴, Y. Hori¹¹³, P. Hristov²⁹, I. Hřivnáčová⁴², M. Huang¹⁴, T.J. Humanic^{15,*}, D.S. Hwang¹⁶, R. Ichou⁶³, R. Ilkaev⁸⁷, I. Ilkiv¹⁰⁰, M. Inaba¹¹⁴, E. Incani¹⁸, G.M. Innocenti²⁵, P.G. Innocenti²⁹, M. Ippolitov⁸⁸, M. Irfan¹³, C. Ivan⁸⁵, V. Ivanov⁷⁵, M. Ivanov⁸⁵, A. Ivanov¹¹⁷, O. Ivanytskyi², A. Jachołkowski²⁹, P.M. Jacobs⁶⁷, H.J. Jang⁶², M.A. Janik¹¹⁸, R. Janik³², P.H.S.Y. Jayarathna¹¹⁰, S. Jena⁴⁰, D.M. Jha¹¹⁹, R.T. Jimenez Bustamante⁵⁵, L. Jirden²⁹, P.G. Jones⁹⁰, H. Jung³⁶, A. Jusko⁹⁰, A.B. Kaidalov⁴⁶, V. Kakoyan¹²¹, S. Kalcher³⁵, P. Kaliňák⁴⁷, T. Kalliokoski³⁷, A. Kalweit⁵³, K. Kanaki¹⁴, J.H. Kang¹²³, V. Kaplin⁶⁹, A. Karasu Uysal^{29,122}, O. Karavichev⁴⁴, T. Karavicheva⁴⁴, E. Karpechev⁴⁴, A. Kazantsev⁸⁸, U. Kebschull⁵¹, R. Keidel¹²⁴, S.A. Khan¹¹⁶, M.M. Khan¹³, P. Khan⁸⁹, A. Khanzadeev⁷⁵, Y. Kharlov⁴³, B. Kileng³¹, T. Kim¹²³, D.W. Kim³⁶, J.H. Kim¹⁶, J.S. Kim³⁶, M. Kim³⁶, B. Kim¹²³, M. Kim¹²³, S.H. Kim³⁶, S. Kim¹⁶, D.J. Kim³⁷, S. Kirsch³⁵, I. Kisiel³⁵, S. Kiselev⁴⁶, A. Kisiel^{29,118}, J.L. Klay⁴, J. Klein⁸², C. Klein-Bösing⁵⁴, M. Kliemant⁵², A. Kluge²⁹, M.L. Knichel⁸⁵, A.G. Knospe¹⁰⁵, K. Koch⁸², M.K. Köhler⁸⁵, A. Kolojvari¹¹⁷, V. Kondratiev¹¹⁷, N. Kondratyeva⁶⁹, A. Konevskikh⁴⁴, A. Korneev⁸⁷, R. Kour⁹⁰, M. Kowalski¹⁰⁴, S. Kox⁶⁴, G. Koyithatta Meethaleveedu⁴⁰, J. Kral³⁷, I. Králik⁴⁷, F. Kramer⁵², I. Kraus⁸⁵, T. Krawutschke^{82,30}, M. Krelina³³, M. Kretz³⁵, M. Krivda^{90,47}, F. Krizek³⁷, M. Krus³³, E. Kryshen⁷⁵, M. Krzewicki⁸⁵, Y. Kucheriaev⁸⁸, C. Kuhn⁵⁸, P.G. Kuijer⁷², I. Kulakov⁵², J. Kumar⁴⁰, P. Kurashvili¹⁰⁰, A. Kurepin⁴⁴, A.B. Kurepin⁴⁴, A. Kuryakin⁸⁷, V. Kushpil⁷³, S. Kushpil⁷³, H. Kvaerno¹⁷, M.J. Kweon⁸², Y. Kwon¹²³, P. Ladrón de Guevara⁵⁵, I. Lakomov⁴², R. Langoy¹⁴, S.L. La Pointe⁴⁵, C. Lara⁵¹, A. Lardeux¹⁰², P. La Rocca²³, C. Lazzeroni⁹⁰, R. Lea²⁰, Y. Le Bornec⁴², M. Lechman²⁹, S.C. Lee³⁶, G.R. Lee⁹⁰, K.S. Lee³⁶, F. Lefèvre¹⁰², J. Lehnert⁵², L. Leistam²⁹, M. Lenhardt¹⁰², V. Lenti⁹⁸, H. León⁵⁶, M. Leoncino⁹⁴, I. León Monzón¹⁰⁶, H. León Vargas⁵², P. Lévai⁶⁰, J. Lien¹⁴, R. Lietava⁹⁰, S. Lindal¹⁷, V. Lindenstruth³⁵, C. Lippmann^{85,29}, M.A. Lisa¹⁵, L. Liu¹⁴, P.I. Loenne¹⁴, V.R. Loggins¹¹⁹, V. Loginov⁶⁹, S. Lohn²⁹, D. Lohner⁸², C. Loizides⁶⁷, K.K. Loo³⁷, X. Lopez⁶³, E. López Torres⁶, G. Løvhøiden¹⁷, X.-G. Lu⁸², P. Luettig⁵², M. Lunardon¹⁹, J. Luo³⁹, G. Luparello⁴⁵, L. Luquin¹⁰², C. Luzzi²⁹, R. Ma¹²⁰, K. Ma³⁹, D.M. Madagodahettige-Don¹¹⁰, A. Maevskaya⁴⁴, M. Mager^{53,29}, D.P. Mahapatra⁴⁸, A. Maire⁸², M. Malaev⁷⁵, I. Maldonado Cervantes⁵⁵, L. Malinina^{59,i}, D. Mal'Kevich⁴⁶, P. Malzacher⁸⁵, A. Mamonov⁸⁷, L. Manceau⁹⁴, L. Mangotra⁸⁰, V. Manko⁸⁸, F. Manso⁶³, V. Manzari⁹⁸, Y. Mao³⁹, M. Marchisone^{63,25}, J. Mareš⁴⁹, G.V. Margagliotti^{20,92}, A. Margotti⁹⁷, A. Marín⁸⁵, C.A. Marin Tobon²⁹, C. Markert¹⁰⁵, I. Martashvili¹¹², P. Martinengo²⁹, M.I. Martínez¹, A. Martínez Davalos⁵⁶, G. Martínez García¹⁰², Y. Martynov², A. Mas¹⁰², S. Masciocchi⁸⁵, M. Masera²⁵, A. Masoni⁹⁶, L. Massacrier^{109,102}, M. Mastromarco⁹⁸, A. Mastroserio^{27,29}, Z.L. Matthews⁹⁰, A. Matyja^{104,102}, D. Mayani⁵⁵, C. Mayer¹⁰⁴, J. Mazer¹¹², M.A. Mazzoni⁹⁵, F. Meddi²², A. Menchaca-Rocha⁵⁶, J. Mercado Pérez⁸², M. Meres³², Y. Miake¹¹⁴, L. Milano²⁵, J. Milosevic¹⁷, A. Mischke⁴⁵, A.N. Mishra⁸¹, D. Miśkowiec^{85,29}, C. Mitu⁵⁰, J. Mlynarz¹¹⁹, B. Mohanty¹¹⁶, A.K. Mohanty²⁹, L. Molnar²⁹, L. Montaño Zetina⁸, M. Monteno⁹⁴, E. Montes⁷, T. Moon¹²³, M. Morando¹⁹, D.A. Moreira De Godoy¹⁰⁷, S. Moretto¹⁹, A. Morsch²⁹, V. Muccifora⁶⁵, E. Mudnic¹⁰³, S. Muhuri¹¹⁶, M. Mukherjee¹¹⁶, H. Müller²⁹, M.G. Munhoz¹⁰⁷, L. Musa²⁹, A. Musso⁹⁴, B.K. Nandi⁴⁰, R. Nania⁹⁷, E. Nappi⁹⁸, C. Natrass¹¹², N.P. Naumov⁸⁷, S. Navin⁹⁰, T.K. Nayak¹¹⁶, S. Nazarenko⁸⁷, G. Nazarov⁸⁷, A. Nedosekin⁴⁶, M. Niculescu^{50,29}, B.S. Nielsen⁷¹, T. Niida¹¹⁴, S. Nikolaev⁸⁸, V. Nikolic⁸⁶, S. Nikulin⁸⁸, V. Nikulin⁷⁵, B.S. Nilsen⁷⁶, M.S. Nilsson¹⁷, F. Noferini^{97,9}, P. Nomokonov⁵⁹, G. Nooren⁴⁵, N. Novitzky³⁷, A. Nyanin⁸⁸, A. Nyatha⁴⁰, C. Nygaard⁷¹, J. Nystrand¹⁴, A. Ochirov¹¹⁷, H. Oeschler^{53,29}, S. Oh¹²⁰, S.K. Oh³⁶, J. Oleniacz¹¹⁸, C. Oppedisano⁹⁴, A. Ortiz Velasquez^{28,55}, G. Ortona²⁵, A. Oskarsson²⁸, P. Ostrowski¹¹⁸, J. Otwinowski⁸⁵, K. Oyama⁸², K. Ozawa¹¹³, Y. Pachmayer⁸², M. Pachr³³, F. Padilla²⁵, P. Pagano²⁴, G. Paić⁵⁵, F. Painke³⁵, C. Pajares¹², S. Pal¹¹, S.K. Pal¹¹⁶, A. Palaha⁹⁰, A. Palmeri⁹⁹, V. Papikyan¹²¹, G.S. Pappalardo⁹⁹, W.J. Park⁸⁵, A. Passfeld⁵⁴, B. Pastircák⁴⁷, D.I. Patalakha⁴³, V. Paticchio⁹⁸, A. Pavlinov¹¹⁹, T. Pawlak¹¹⁸, T. Peitzmann⁴⁵, H. Pereira Da Costa¹¹, E. Pereira De Oliveira Filho¹⁰⁷, D. Peresunko⁸⁸, C.E. Pérez Lara⁷², E. Perez Lezama⁵⁵, D. Perini²⁹, D. Perrino²⁷, W. Peryt¹¹⁸, A. Pesci⁹⁷, V. Peskov^{29,55}, Y. Pestov³, V. Petráček³³, M. Petran³³, M. Petris⁷⁰, P. Petrov⁹⁰, M. Petrovici⁷⁰, C. Petta²³, S. Piano⁹², A. Piccotti⁹⁴, M. Pikna³², P. Pillot¹⁰², O. Pinazza²⁹, L. Pinsky¹¹⁰, N. Pitz⁵², D.B. Piyarathna¹¹⁰, M. Płoskoń⁶⁷, J. Pluta¹¹⁸, T. Pocheptsov⁵⁹, S. Pochybova⁶⁰, P.L.M. Podesta-Lerma¹⁰⁶, M.G. Poghosyan^{29,25}, K. Polák⁴⁹, B. Polichtchouk⁴³, A. Pop⁷⁰, S. Porteboeuf-Houssais⁶³, V. Pospíšil³³, B. Potukuchi⁸⁰, S.K. Prasad¹¹⁹, R. Preghenella^{97,9}, F. Prino⁹⁴, C.A. Pruneau¹¹⁹, I. Pshenichnov⁴⁴,

- S. Puchagin ⁸⁷, G. Puddu ¹⁸, J. Pujol Teixido ⁵¹, A. Pulvirenti ^{23,29}, V. Punin ⁸⁷, M. Putiš ³⁴,
 J. Putschke ^{119,120}, E. Quercigh ²⁹, H. Qvigstad ¹⁷, A. Rachevski ⁹², A. Rademakers ²⁹, S. Radomski ⁸²,
 T.S. Räihä ³⁷, J. Rak ³⁷, A. Rakotozafindrabe ¹¹, L. Ramello ²⁶, A. Ramírez Reyes ⁸, S. Raniwala ⁸¹,
 R. Raniwala ⁸¹, S.S. Räsänen ³⁷, B.T. Rascanu ⁵², D. Rathee ⁷⁷, K.F. Read ¹¹², J.S. Real ⁶⁴, K. Redlich ^{100,57},
 P. Reichelt ⁵², M. Reicher ⁴⁵, R. Renfordt ⁵², A.R. Reolon ⁶⁵, A. Reshetin ⁴⁴, F. Rettig ³⁵, J.-P. Revol ²⁹,
 K. Reygers ⁸², L. Riccati ⁹⁴, R.A. Ricci ⁶⁶, T. Richert ²⁸, M. Richter ¹⁷, P. Riedler ²⁹, W. Riegler ²⁹,
 F. Riggi ^{23,99}, B. Rodrigues Fernandes Rabacal ²⁹, M. Rodríguez Cahuantzi ¹, A. Rodriguez Manso ⁷²,
 K. Røed ¹⁴, D. Rohr ³⁵, D. Röhrich ¹⁴, R. Romita ⁸⁵, F. Ronchetti ⁶⁵, P. Rosnet ⁶³, S. Rossegger ²⁹,
 A. Rossi ^{29,19}, C. Roy ⁵⁸, P. Roy ⁸⁹, A.J. Rubio Montero ⁷, R. Rui ²⁰, E. Ryabinkin ⁸⁸, A. Rybicki ¹⁰⁴,
 S. Sadovsky ⁴³, K. Šafařík ²⁹, R. Sahoo ⁴¹, P.K. Sahu ⁴⁸, J. Saini ¹¹⁶, H. Sakaguchi ³⁸, S. Sakai ⁶⁷, D. Sakata ¹¹⁴,
 C.A. Salgado ¹², J. Salzwedel ¹⁵, S. Sambyal ⁸⁰, V. Samsonov ⁷⁵, X. Sanchez Castro ⁵⁸, L. Šádor ⁴⁷,
 A. Sandoval ⁵⁶, S. Sano ¹¹³, M. Sano ¹¹⁴, R. Santo ⁵⁴, R. Santoro ^{98,29,9}, J. Sarkamo ³⁷, E. Scapparone ⁹⁷,
 F. Scarlassara ¹⁹, R.P. Scharenberg ⁸³, C. Schiaua ⁷⁰, R. Schicker ⁸², C. Schmidt ⁸⁵, H.R. Schmidt ¹¹⁵,
 S. Schreiner ²⁹, S. Schuchmann ⁵², J. Schukraft ²⁹, Y. Schutz ^{29,102}, K. Schwarz ⁸⁵, K. Schweda ^{85,82},
 G. Scioli ²¹, E. Scomparin ⁹⁴, R. Scott ¹¹², P.A. Scott ⁹⁰, G. Segato ¹⁹, I. Selyuzhenkov ⁸⁵, S. Senyukov ^{26,58},
 J. Seo ⁸⁴, S. Serci ¹⁸, E. Serradilla ^{7,56}, A. Sevcenco ⁵⁰, A. Shabetai ¹⁰², G. Shabratova ⁵⁹, R. Shahoyan ²⁹,
 N. Sharma ⁷⁷, S. Sharma ⁸⁰, S. Rohni ⁸⁰, K. Shigaki ³⁸, M. Shimomura ¹¹⁴, K. Shtejer ⁶, Y. Sibiriak ⁸⁸,
 M. Siciliano ²⁵, E. Sicking ²⁹, S. Siddhanta ⁹⁶, T. Siemianczuk ¹⁰⁰, D. Silvermyr ⁷⁴, C. Silvestre ⁶⁴,
 G. Simatovic ⁸⁶, G. Simonetti ²⁹, R. Singaraju ¹¹⁶, R. Singh ⁸⁰, S. Singha ¹¹⁶, V. Singhal ¹¹⁶, T. Sinha ⁸⁹,
 B.C. Sinha ¹¹⁶, B. Sitar ³², M. Sitta ²⁶, T.B. Skaali ¹⁷, K. Skjerdal ¹⁴, R. Smakal ³³, N. Smirnov ¹²⁰,
 R.J.M. Snellings ⁴⁵, C. Søgaard ⁷¹, R. Soltz ⁶⁸, H. Son ¹⁶, M. Song ¹²³, J. Song ⁸⁴, C. Soos ²⁹, F. Soramel ¹⁹,
 I. Sputowska ¹⁰⁴, M. Spyropoulou-Stassinaki ⁷⁸, B.K. Srivastava ⁸³, J. Stachel ⁸², I. Stan ⁵⁰, I. Stan ⁵⁰,
 G. Stefanek ¹⁰⁰, T. Steinbeck ³⁵, M. Steinpreis ¹⁵, E. Stenlund ²⁸, G. Steyn ⁷⁹, J.H. Stiller ⁸², D. Stocco ¹⁰²,
 M. Stolpovskiy ⁴³, K. Strabykin ⁸⁷, P. Strmen ³², A.A.P. Suaiide ¹⁰⁷, M.A. Subieta Vásquez ²⁵, T. Sugitate ³⁸,
 C. Suire ⁴², M. Sukhorukov ⁸⁷, R. Sultanov ⁴⁶, M. Šumbera ⁷³, T. Susa ⁸⁶, A. Szanto de Toledo ¹⁰⁷,
 I. Szarka ³², A. Szccepankiewicz ^{104,29}, A. Szostak ¹⁴, M. Szymanski ¹¹⁸, J. Takahashi ¹⁰⁸,
 J.D. Tapia Takaki ⁴², A. Tauro ²⁹, G. Tejeda Muñoz ¹, A. Telesca ²⁹, C. Terrevoli ²⁷, J. Thäder ⁸⁵, D. Thomas ⁴⁵,
 R. Tieulent ¹⁰⁹, A.R. Timmins ¹¹⁰, D. Tlusty ³³, A. Toia ^{35,29}, H. Torii ¹¹³, L. Toscano ⁹⁴, D. Truesdale ¹⁵,
 W.H. Trzaska ³⁷, T. Tsuji ¹¹³, A. Tumkin ⁸⁷, R. Turrisi ⁹³, T.S. Tveter ¹⁷, J. Ulery ⁵², K. Ullaland ¹⁴,
 J. Ulrich ^{61,51}, A. Uras ¹⁰⁹, J. Urbán ³⁴, G.M. Urciuoli ⁹⁵, G.L. Usai ¹⁸, M. Vajzer ^{33,73}, M. Vala ^{59,47},
 L. Valencia Palomo ⁴², S. Vallero ⁸², N. van der Kolk ⁷², P. Vande Vyvre ²⁹, M. van Leeuwen ⁴⁵,
 L. Vannucci ⁶⁶, A. Vargas ¹, R. Varma ⁴⁰, M. Vasileiou ⁷⁸, A. Vasiliev ⁸⁸, V. Vechernin ¹¹⁷, M. Veldhoen ⁴⁵,
 M. Venaruzzo ²⁰, E. Vercellin ²⁵, S. Vergara ¹, R. Vernet ⁵, M. Verweij ⁴⁵, L. Vickovic ¹⁰³, G. Viesti ¹⁹,
 O. Vikhlyantsev ⁸⁷, Z. Vilakazi ⁷⁹, O. Villalobos Baillie ⁹⁰, A. Vinogradov ⁸⁸, L. Vinogradov ¹¹⁷,
 Y. Vinogradov ⁸⁷, T. Virgili ²⁴, Y.P. Viyogi ¹¹⁶, A. Vodopyanov ⁵⁹, K. Voloshin ⁴⁶, S. Voloshin ¹¹⁹,
 G. Volpe ^{27,29}, B. von Haller ²⁹, D. Vranic ⁸⁵, G. Øvrebekk ¹⁴, J. Vrláková ³⁴, B. Vulpescu ⁶³, A. Vyushin ⁸⁷,
 V. Wagner ³³, B. Wagner ¹⁴, R. Wan ³⁹, M. Wang ³⁹, D. Wang ³⁹, Y. Wang ⁸², Y. Wang ³⁹, K. Watanabe ¹¹⁴,
 M. Weber ¹¹⁰, J.P. Wessels ^{29,54}, U. Westerhoff ⁵⁴, J. Wiechula ¹¹⁵, J. Wikne ¹⁷, M. Wilde ⁵⁴, G. Wilk ¹⁰⁰,
 A. Wilk ⁵⁴, M.C.S. Williams ⁹⁷, B. Windelband ⁸², L. Xaplanteris Karampatsos ¹⁰⁵, C.G. Yaldo ¹¹⁹,
 Y. Yamaguchi ¹¹³, H. Yang ¹¹, S. Yang ¹⁴, S. Yasnopolskiy ⁸⁸, J. Yi ⁸⁴, Z. Yin ³⁹, I.-K. Yoo ⁸⁴, J. Yoon ¹²³,
 W. Yu ⁵², X. Yuan ³⁹, I. Yushmanov ⁸⁸, C. Zach ³³, C. Zampolli ⁹⁷, S. Zaporozhets ⁵⁹, A. Zarochentsev ¹¹⁷,
 P. Závada ⁴⁹, N. Zaviyalov ⁸⁷, H. Zbroszczyk ¹¹⁸, P. Zelnicek ⁵¹, I.S. Zgura ⁵⁰, M. Zhalov ⁷⁵, X. Zhang ^{63,39},
 H. Zhang ³⁹, F. Zhou ³⁹, D. Zhou ⁴⁵, Y. Zhou ³⁹, J. Zhu ³⁹, X. Zhu ³⁹, A. Zichichi ^{21,9},
 A. Zimmermann ⁸², G. Zinovjev ², Y. Zoccarato ¹⁰⁹, M. Zynovyyev ², M. Zyzak ⁵²

¹ Benemérita Universidad Autónoma de Puebla, Puebla, Mexico² Bogolyubov Institute for Theoretical Physics, Kiev, Ukraine³ Budker Institute for Nuclear Physics, Novosibirsk, Russia⁴ California Polytechnic State University, San Luis Obispo, CA, United States⁵ Centre de Calcul de l'IN2P3, Villeurbanne, France⁶ Centro de Aplicaciones Tecnológicas y Desarrollo Nuclear (CEADEN), Havana, Cuba⁷ Centro de Investigaciones Energéticas Medioambientales y Tecnológicas (CIEMAT), Madrid, Spain⁸ Centro de Investigación y de Estudios Avanzados (CINVESTAV), Mexico City and Mérida, Mexico⁹ Centro Fermi – Centro Studi e Ricerche e Museo Storico della Física "Enrico Fermi", Rome, Italy¹⁰ Chicago State University, Chicago, IL, United States¹¹ Commissariat à l'Energie Atomique, IRFU, Saclay, France¹² Departamento de Física de Partículas and IGFAE, Universidad de Santiago de Compostela, Santiago de Compostela, Spain

- ¹³ Department of Physics Aligarh Muslim University, Aligarh, India
¹⁴ Department of Physics and Technology, University of Bergen, Bergen, Norway
¹⁵ Department of Physics, Ohio State University, Columbus, OH, United States
¹⁶ Department of Physics, Sejong University, Seoul, South Korea
¹⁷ Department of Physics, University of Oslo, Oslo, Norway
¹⁸ Dipartimento di Fisica dell'Università and Sezione INFN, Cagliari, Italy
¹⁹ Dipartimento di Fisica dell'Università and Sezione INFN, Padova, Italy
²⁰ Dipartimento di Fisica dell'Università and Sezione INFN, Trieste, Italy
²¹ Dipartimento di Fisica dell'Università and Sezione INFN, Bologna, Italy
²² Dipartimento di Fisica dell'Università 'La Sapienza' and Sezione INFN, Rome, Italy
²³ Dipartimento di Fisica e Astronomia dell'Università and Sezione INFN, Catania, Italy
²⁴ Dipartimento di Fisica 'E.R. Caianiello' dell'Università and Gruppo Collegato INFN, Salerno, Italy
²⁵ Dipartimento di Fisica Sperimentale dell'Università and Sezione INFN, Turin, Italy
²⁶ Dipartimento di Scienze e Innovazione Tecnologica dell'Università del Piemonte Orientale and Gruppo Collegato INFN, Alessandria, Italy
²⁷ Dipartimento Interateneo di Fisica 'M. Merlin' and Sezione INFN, Bari, Italy
²⁸ Division of Experimental High Energy Physics, University of Lund, Lund, Sweden
²⁹ European Organization for Nuclear Research (CERN), Geneva, Switzerland
³⁰ Fachhochschule Köln, Köln, Germany
³¹ Faculty of Engineering, Bergen University College, Bergen, Norway
³² Faculty of Mathematics, Physics and Informatics, Comenius University, Bratislava, Slovakia
³³ Faculty of Nuclear Sciences and Physical Engineering, Czech Technical University in Prague, Prague, Czech Republic
³⁴ Faculty of Science, P.J. Šafárik University, Košice, Slovakia
³⁵ Frankfurt Institute for Advanced Studies, Johann Wolfgang Goethe-Universität Frankfurt, Frankfurt, Germany
³⁶ Gangneung-Wonju National University, Gangneung, South Korea
³⁷ Helsinki Institute of Physics (HIP) and University of Jyväskylä, Jyväskylä, Finland
³⁸ Hiroshima University, Hiroshima, Japan
³⁹ Hua-Zhong Normal University, Wuhan, China
⁴⁰ Indian Institute of Technology, Mumbai, India
⁴¹ Indian Institute of Technology Indore (IIT), Indore, India
⁴² Institut de Physique Nucléaire d'Orsay (IPNO), Université Paris-Sud, CNRS-IN2P3, Orsay, France
⁴³ Institute for High Energy Physics, Protvino, Russia
⁴⁴ Institute for Nuclear Research, Academy of Sciences, Moscow, Russia
⁴⁵ Nikhef, National Institute for Subatomic Physics and Institute for Subatomic Physics of Utrecht University, Utrecht, Netherlands
⁴⁶ Institute for Theoretical and Experimental Physics, Moscow, Russia
⁴⁷ Institute of Experimental Physics, Slovak Academy of Sciences, Košice, Slovakia
⁴⁸ Institute of Physics, Bhubaneswar, India
⁴⁹ Institute of Physics, Academy of Sciences of the Czech Republic, Prague, Czech Republic
⁵⁰ Institute of Space Sciences (ISS), Bucharest, Romania
⁵¹ Institut für Informatik, Johann Wolfgang Goethe-Universität Frankfurt, Frankfurt, Germany
⁵² Institut für Kernphysik, Johann Wolfgang Goethe-Universität Frankfurt, Frankfurt, Germany
⁵³ Institut für Kernphysik, Technische Universität Darmstadt, Darmstadt, Germany
⁵⁴ Institut für Kernphysik, Westfälische Wilhelms-Universität Münster, Münster, Germany
⁵⁵ Instituto de Ciencias Nucleares, Universidad Nacional Autónoma de México, Mexico City, Mexico
⁵⁶ Instituto de Física, Universidad Nacional Autónoma de México, Mexico City, Mexico
⁵⁷ Institute of Theoretical Physics, University of Wroclaw, Poland
⁵⁸ Institut Pluridisciplinaire Hubert Curien (IPHC), Université de Strasbourg, CNRS-IN2P3, Strasbourg, France
⁵⁹ Joint Institute for Nuclear Research (JINR), Dubna, Russia
⁶⁰ KFKI Research Institute for Particle and Nuclear Physics, Hungarian Academy of Sciences, Budapest, Hungary
⁶¹ Kirchhoff-Institut für Physik, Ruprecht-Karls-Universität Heidelberg, Heidelberg, Germany
⁶² Korea Institute of Science and Technology Information, Daejeon, South Korea
⁶³ Laboratoire de Physique Corpusculaire (LPC), Clermont Université, Université Blaise Pascal, CNRS-IN2P3, Clermont-Ferrand, France
⁶⁴ Laboratoire de Physique Subatomique et de Cosmologie (LPSC), Université Joseph Fourier, CNRS-IN2P3, Institut Polytechnique de Grenoble, Grenoble, France
⁶⁵ Laboratori Nazionali di Frascati, INFN, Frascati, Italy
⁶⁶ Laboratori Nazionali di Legnaro, INFN, Legnaro, Italy
⁶⁷ Lawrence Berkeley National Laboratory, Berkeley, CA, United States
⁶⁸ Lawrence Livermore National Laboratory, Livermore, CA, United States
⁶⁹ Moscow Engineering Physics Institute, Moscow, Russia
⁷⁰ National Institute for Physics and Nuclear Engineering, Bucharest, Romania
⁷¹ Niels Bohr Institute, University of Copenhagen, Copenhagen, Denmark
⁷² Nikhef, National Institute for Subatomic Physics, Amsterdam, Netherlands
⁷³ Nuclear Physics Institute, Academy of Sciences of the Czech Republic, Řež u Prahy, Czech Republic
⁷⁴ Oak Ridge National Laboratory, Oak Ridge, TN, United States
⁷⁵ Petersburg Nuclear Physics Institute, Gatchina, Russia
⁷⁶ Physics Department, Creighton University, Omaha, NE, United States
⁷⁷ Physics Department, Panjab University, Chandigarh, India
⁷⁸ Physics Department, University of Athens, Athens, Greece
⁷⁹ Physics Department, University of Cape Town, iThemba LABS, Cape Town, South Africa
⁸⁰ Physics Department, University of Jammu, Jammu, India
⁸¹ Physics Department, University of Rajasthan, Jaipur, India
⁸² Physikalisches Institut, Ruprecht-Karls-Universität Heidelberg, Heidelberg, Germany
⁸³ Purdue University, West Lafayette, IN, United States
⁸⁴ Pusan National University, Pusan, South Korea
⁸⁵ Research Division and ExtreMe Matter Institute EMMI, GSI Helmholtzzentrum für Schwerionenforschung, Darmstadt, Germany
⁸⁶ Rudjer Bošković Institute, Zagreb, Croatia
⁸⁷ Russian Federal Nuclear Center (VNIIEF), Sarov, Russia
⁸⁸ Russian Research Centre Kurchatov Institute, Moscow, Russia
⁸⁹ Saha Institute of Nuclear Physics, Kolkata, India
⁹⁰ School of Physics and Astronomy, University of Birmingham, Birmingham, United Kingdom
⁹¹ Sección Física, Departamento de Ciencias, Pontificia Universidad Católica del Perú, Lima, Peru

- ⁹² Sezione INFN, Trieste, Italy
⁹³ Sezione INFN, Padova, Italy
⁹⁴ Sezione INFN, Turin, Italy
⁹⁵ Sezione INFN, Rome, Italy
⁹⁶ Sezione INFN, Cagliari, Italy
⁹⁷ Sezione INFN, Bologna, Italy
⁹⁸ Sezione INFN, Bari, Italy
⁹⁹ Sezione INFN, Catania, Italy
¹⁰⁰ Soltan Institute for Nuclear Studies, Warsaw, Poland
¹⁰¹ Nuclear Physics Group, STFC Daresbury Laboratory, Daresbury, United Kingdom
¹⁰² SUBATECH, Ecole des Mines de Nantes, Université de Nantes, CNRS-IN2P3, Nantes, France
¹⁰³ Technical University of Split FESB, Split, Croatia
¹⁰⁴ The Henryk Niewodniczanski Institute of Nuclear Physics, Polish Academy of Sciences, Cracow, Poland
¹⁰⁵ The University of Texas at Austin, Physics Department, Austin, TX, United States
¹⁰⁶ Universidad Autónoma de Sinaloa, Culiacán, Mexico
¹⁰⁷ Universidade de São Paulo (USP), São Paulo, Brazil
¹⁰⁸ Universidade Estadual de Campinas (UNICAMP), Campinas, Brazil
¹⁰⁹ Université de Lyon, Université Lyon 1, CNRS/IN2P3, IPN-Lyon, Villeurbanne, France
¹¹⁰ University of Houston, Houston, TX, United States
¹¹¹ University of Technology and Austrian Academy of Sciences, Vienna, Austria
¹¹² University of Tennessee, Knoxville, TN, United States
¹¹³ University of Tokyo, Tokyo, Japan
¹¹⁴ University of Tsukuba, Tsukuba, Japan
¹¹⁵ Eberhard Karls Universität Tübingen, Tübingen, Germany
¹¹⁶ Variable Energy Cyclotron Centre, Kolkata, India
¹¹⁷ V. Fock Institute for Physics, St. Petersburg State University, St. Petersburg, Russia
¹¹⁸ Warsaw University of Technology, Warsaw, Poland
¹¹⁹ Wayne State University, Detroit, MI, United States
¹²⁰ Yale University, New Haven, CT, United States
¹²¹ Yerevan Physics Institute, Yerevan, Armenia
¹²² Yildiz Technical University, Istanbul, Turkey
¹²³ Yonsei University, Seoul, South Korea
¹²⁴ Zentrum für Technologietransfer und Telekommunikation (ZTT), Fachhochschule Worms, Worms, Germany

* Corresponding author.

E-mail address: humanic@mps.ohio-state.edu (T.J. Humanic).

ⁱ Also at: M.V. Lomonosov Moscow State University, D.V. Skobeltsyn Institute of Nuclear Physics, Moscow, Russia.